Optimizing Stopes and Rib Pillars in Sublevel Open Stoping Mining Method: An Automated Numerical Modeling Approach

Diogo Peixoto Cordova
Professor, Federal University of Rio Grande do Sul, Porto Alegre, Brazil, diogo.cordova@ufrgs.br

Ítalo Gomes Gonçalves
Professor, Federal University of Pampa, Caçapava do Sul, Brazil, italogoncalves@unipampa.edu.br

Andre Cezar Zingano
Professor, Federal University of Rio Grande do Sul, Porto Alegre, Brazil, andrezin@ufrgs.br

ABSTRACT: The top-down extraction sequence in the sublevel open stope method leaves rib pillars to support the excavations, making dilution control critical. This study introduces an integrated methodology for optimizing net profit and geomechanical performance of open stope layouts and rib pillars using a genetic algorithm. User-informed parameters such as minimum stope size, minimum pillar size, maximum accepted dilution, and maximum acceptable percentage of pillar failure are considered. A graphical user interface (GUI) was created to make its application easier. A profit function, capable of assigning economic value to the analyzed geometric configuration, including geomechanical performance, is developed. Geomechanical performance of the geometric configurations is determined through autonomous numerical models in FLAC3D software, which include average percentage of pillar failure and potential dilution. The algorithm's validity is demonstrated through a case study involving a mining panel in an underground gold mine. An 8% increase in net profit relative to the engineer's design method was achieved, assuming 70% hangingwall support efficiency for both methods. Pillar failure percentage decreased threefold. When no HW support is considered, the net profit increase is 22% compared to the engineer's design method. This methodology showcases the feasibility of integrated optimization, considering mining costs and geomechanical performance costs, thereby reducing the need for secondary support.

KEYWORDS: stope optimization, dilution, hangingwall, pillar failure, FLAC3D

1   INTRODUCTION

The sublevel open stope (SLOS) involves ore extraction through the creation of sizable stopes separated by sublevels, crown, and rib pillars. These stopes are excavated parallel to the ore body's strike, leaving vertical pillars for support. Extraction progresses by retreating from the sides towards the center, following a top-down approach starting from upper levels and moving downwards while working on sublevels simultaneously. Long-term planning for SLOS typically entails determining sublevel spacing, maximum stope spans, and sizing of rib, sill, and crown pillars. Layout and sequencing are then validated using numerical models to ensure stress redistribution, assess dilution in the hangingwall and evaluate overall stability.

However, this method may introduce inefficiencies due to generalized pillar and stope sizes, which can vary given variations in rock mass properties like dip angles and thickness. Thus, an irregular arrangement of stopes and pillars could yield a more optimized geometry, enhancing profitability. This optimization involves placing pillars in areas with lower grades or waste, thereby reducing potential dilution in stopes.

This study aims to propose an integrated methodology for economically and geomechanically optimizing open stope and vertical rib pillar layouts. It includes developing an evolutionary algorithm considering criteria like minimum stope and pillar size, maximum dilution, and acceptable pillar failure.

2   THEORY AND BACKGROUND

2.1 Genetic Algorithms

XX ICongresso Brasileiro de Mecânica dos Solos e Engenharia Geotécnica
X Simpósio Brasileiro de Mecânica das Rochas
X Simpósio Brasileiro de Engenheiros Geotécnicos Jovens
24 a 27 de setembro de 2024 – Balneário Camboriú/SC

COBRAMSEG 2024
XXI Congresso Brasileiro de Mecânica dos Solos e Eng. Geotécnica
X Simpósio Brasileiro de Mecânica das Rochas
X Simpósio Brasileiro de Engenheiros Geotécnicos Jovens

Genetic algorithms (GAs) iteratively refine a population of candidates until the problem's solution is reached, employing operators inspired by genetic variation and natural selection. Unlike some algorithms confined to exploring solutions in a single space, GAs can traverse multiple directions simultaneously. This versatility allows them to swiftly discard unpromising paths and pivot towards more favorable directions, avoiding stagnation and repetitive starts. Key components typically found in GAs include a diverse population of individuals with unique chromosomes, selection based on fitness, crossover for generating new generations, and introducing random mutations in subsequent iterations (Mitchell, 1998).

2.2 Optimization algorithms

Over time, multiple methods have emerged to enhance the economic efficiency of stopes; however, each has inherent shortcomings that hinder widespread adoption and reliability. Among the most prevalent algorithms is the heuristic approach known as Floating Stope (Alford, 2006). This method utilizes input parameters such as sublevel spacing, stope dimensions, pillar sizes, wall contact dilution, cutoff grade, and dip angles for hangingwall (HW) and footwall (FW).

Recent research efforts have aimed to optimize both pillars and stopes. While some studies concentrate solely on geomechanical enhancements, others endeavor to integrate economic considerations using diverse methodologies such as numerical modeling, neural networks, genetic algorithms, or mathematical optimization equations (Napa-Garcia et al, 2019; Heidarzadeh et al, 2019; Sari and Kumral, 2020).

3 METHODOLOGY

The algorithm's development involves Python scripting for the genetic algorithm, profit function, and interfacing with FLAC3D for automated numerical modeling. Initially, the case study files undergo importing into Micromine software, which optimizes the economic boundaries of the stopes. These boundaries are then segmented into vertical slices, each 1 meter thick along the mineralized body's strike axis, resulting in closed wireframe volumes. The gold grade for each slice is determined using the available block model. Subsequently, the initial population is generated through stochastic simulation, with each individual representing a configuration of stopes and pillars. The algorithm scans each sublevel, user-defined, creating alternating arrangements of stopes and pillars based on selected slices while adhering to size constraints. These individuals are then subjected to numerical analysis in FLAC3D.

Next, each individual undergoes evaluation via the fitness function, which assigns a net profit. The genetic algorithm commences by randomly selecting individuals from the population to reproduce, generating offspring with shared genetic characteristics. These offspring might undergo mutation to ensure genetic diversity before being evaluated economically using the fitness function. The algorithm iterates by generating new individuals and repeating the steps until reaching the maximum number of user-defined iterations.

3.1 Rock mass failure criteria

Within hard rock mining contexts, the stresses imposed by excavations can trigger deformations, fracture propagation, spalling, or even total collapse. Hence, understanding failure modes is pivotal in evaluating stope stability. Broadly, block falls are typically associated with stress relaxation, primarily observed in the HW of stopes, leading to dilution. Pillars, on the other hand, are prone to sudden failures under conditions of high confinement. These occurrences arise from the redistribution of stresses in situ. Depending on the width-to-height ratio of the pillars, failure mechanisms may involve crushing or shearing, often manifesting as an hourglass shape with edge-initiated failures (Diederichs, 1999; Castro, 2012).

The deviatoric stress is the difference between the maximum and minimum principal stresses and its most common use is through the concept of maximum shear stress. This criterion is often used to assess the effect of stresses induced by excavations in the rock mass, especially in an environment of deep excavations or rocks with brittle behavior (Diederichs, 1999). By using this approach, 2D and 3D numerical elastic models are applied to estimate areas where damage could accumulate and create the potential for abrupt failures around openings due to the high compressive stresses induced (Castro, 2012).

The σ_1' and σ_3' are the calculated effective principal stresses for the element in question and σ'' is the maximum principal stress that the rock can withstand until the moment of failure, keeping a constant σ'. The

XX ICongresso Brasileiro de Mecânica dos Solos e Engenharia Geotécnica
X Simpósio Brasileiro de Mecânica das Rochas
X Simpósio Brasileiro de Engenheiros Geotécnicos Jovens
24 a 27 de setembro de 2024 – Balneário Camboriú/SC

σ'' is a function of the failure envelope of the rock, in the case of the Mohr-Coulomb criterion, the cohesion and the friction angle. A strength-stress ratio (SSR) value close to one indicates that the element has reached its strength limit and is in a state of failure. Equation 1 demonstrates the calculation of the SSR.

$$SSR = \left| \frac{\sigma''_1 - \sigma'_3}{\sigma'_1 - \sigma'_3} \right| \tag{1}$$

Rib pillar performance evaluation relies on the derived SSR values. Typically, the core regions of pillars exhibit SSR values exceeding one, contrasting with the edges where SSR often falls below this threshold. An SSR below one signifies localized stress concentrations leading to failure. Calculating the percentage of pillar failure (PPF) involves dividing the volume of failed numerical elements within pillars by the total pillar element volume.

The presence of tensile stress on excavation surfaces serves as a indicator of HW instability assessment. Given the rock mass's negligible tensile strength, regions experiencing low confinement or tensile stress are prone to gravity-induced failure. When the magnitude of stress σ_3 surpasses the rock mass's tensile strength limit, irrespective of σ_1, the excavation is deemed to have failed (Diederichs, 1999; Cordova et al, 2022).

Following excavation, the numerical model attains a new equilibrium, facilitating the examination of stress redistribution within the HW of stopes. This is observed through the relaxation zone volume in each stope, delineated by stress isovalues of σ_3. A larger relaxation zone indicates heightened HW instability, attributable to reduced confinement, thereby increasing the risk of ore dilution. Consequently, the average potential dilution percentage (D_{model}) is calculated by dividing the volume of HW numerical elements with σ_3 less than zero by the total volume of stopes, galleries, and failed HW elements. To support the HW, cablebolts are employed, and their effectiveness is gauged by the percentage of successfully retained waste material. Subsequently, actual dilution (D_{actual}) is determined based on the HW support's efficacy.

3.2 Net profit function

To calculate the net profit function, which can economically evaluate a geometry set, input parameters are required and are filled in by the user (Table 1). Initially, the gross revenue is calculated in (2).

$$G_{value} = P_r \cdot G_r \cdot M_s \cdot R_1 \cdot R_2 \tag{2}$$

A logical test is performed to calculate the cost of reinforcing pillars in (3).

$$C_{ps} = \begin{cases} C_{ups} \cdot V_{pf}, & PPF > PPF_{max} \\ 0, & PPF \leq PPF_{max} \end{cases} \tag{3}$$

Another logical test is performed to determine the cost with additional secondary support added to the HW in (4).

$$C_{hws} = \begin{cases} C_{uhws} \cdot D_{vol}, & D_{model} > D_{max} \\ 0, & D_{model} \leq D_{max} \end{cases} \tag{4}$$

In turn, considering the efficiency attributed to the additional secondary support added to the HW, the actual dilution will be calculated in (5).

$$D_{actual} = \begin{cases} D_{model} - (D_{model} - D_{max}) \cdot \eta_s, & D_{model} > D_{max} \\ D_{model}, & D_{model} \leq D_{max} \end{cases} \tag{5}$$

The cost calculation is given in (6).

$$C_{total} = \Bigg\{ \Big([M_s \cdot R_1 \cdot (1 + D_{actual})] \cdot [C_m + C_p + C_{ga} + (C_t \cdot D_{tr})] \Big)$$
$$+ (G_r \cdot M_s \cdot R_1 \cdot R_2 \cdot C_{ref}) + (C_{roy} \cdot G_{value}) + C_{ps} + C_{hws} \Bigg\} \tag{6}$$

XX ICongresso Brasileiro de Mecânica dos Solos e Engenharia Geotécnica
X Simpósio Brasileiro de Mecânica das Rochas
X Simpósio Brasileiro de Engenheiros Geotécnicos Jovens
24 a 27 de setembro de 2024 – Balneário Camboriú/SC

Finally, net profit will be calculated as given in (7).

$$N_{profit} = G_{value} - C_{total} \tag{7}$$

Table 1. Input and output parameters

Parameters	Equation symbol
Input parameters	
Gold price (\$/g)	P_r
Mining recovery (%)	R_1
Process recovery (%)	R_2
Max. accepted dilution (%)	D_{max}
Max. accepted failed pillar elements (%)	PPF_{max}
Mining cost (\$/t)	C_m
Transport cost (\$/t/m)	C_t
Process cost (\$/t)	C_p
General & admin. cost (\$/t)	C_{ga}
Gold refining (\$/g)	C_{ref}
Royalties (% gross value)	C_{roy}
Secondary support cost (\$/m^3 of dilution)	C_{uhws}
Secondary support efficiency (%)	η_s
Pillar support cost (\$/m^3 of failed pillar)	C_{ups}
Output parameters	
Average ore grade (g/t)	G_r
Stopes' total mass (t)	M_s
Failed pillar elements (%)	PPF
Failed pillar elements (m^3)	V_{pf}
Potential dilution (%)	D_{model}
Potential dilution (m^3)	D_{vol}
Average transport distance (m)	D_{tr}

3.3 Automated numerical models

FLAC3D software stands as a prevalent tool for numerically modeling various geotechnical challenges, enabling the assessment of rock mass behavior post-excavation. It operates as a three-dimensional, explicit, finite difference program. Material properties are represented by zone elements structured within a 3D grid tailored to user specifications. Linear and nonlinear stress/strain laws are incorporated to govern element responses to boundary conditions (Itasca, 2005).

To facilitate the proposed algorithm's search for an optimal stope and pillar layout, necessitating evaluation and optimization of multiple designs via the genetic algorithm, automated execution of numerical models is imperative, devoid of manual intervention. This entails the sequential activation of pre-written codes in FLAC3D command language and FISH language, orchestrated through a socket connection with the Python console leveraging the Itasca Python library package (Furtney, 2020). This library facilitates Socket network protocol communication between the Python kernel and FLAC3D.

Based on the problem's logical structure, the algorithm is partitioned into two separate blocks. The first block executes only once throughout the entire algorithm, while the second block is recurrently executed at each evaluation of the genetic algorithm. After import the geometries, there is a refinement of discretization in specific zones of interest, including galleries, stopes, pillars, and areas near their intersections. Here, cubic elements generated through the octree method undergo successive division until reaching the predefined minimum dimension of one meter.

Following the model setup, the next phase involves initializing key parameters such as properties, constitutive model, boundary conditions, and in situ stresses. Subsequently, the model undergoes execution to establish initial balance among acting forces before any excavation takes place. In FLAC3D, convergence is typically attained when the average force ratio reaches a value of 10^{-5}. This ratio is computed as the sum of all out-of-balance force components at each grid point divided by the sum of all total applied forces at that point (Itasca, 2005). Upon achieving equilibrium, the model state is saved.

After equilibrium, the model excavates galleries, followed by stopes. Given the algorithm's reliance on

XX ICongresso Brasileiro de Mecânica dos Solos e Engenharia Geotécnica
X Simpósio Brasileiro de Mecânica das Rochas
X Simpósio Brasileiro de Engenheiros Geotécnicos Jovens
24 a 27 de setembro de 2024 – Balneário Camboriú/SC

the Mohr-Coulomb criterion and FLAC3D's default behavior where tensile failure maintains constant tensile strength within a zone, the 'flag-brittle' command is utilized. This command resets tensile strength to zero in zones experiencing tensile failure, facilitating simulation of instantaneous softening due to tensile stress.

Upon reaching the new equilibrium post-excavation, an assessment of tension redistribution within the HW of stopes becomes feasible. This assessment involves observing the volume of the relaxation zone in each stope through σ_3 stress isovalues. A larger relaxation zone signifies heightened HW instability due to confinement loss, thus amplifying the risk of ore dilution.

Pillar performance is evaluated based on the attained SSR. The volume of failed pillar elements, combined with the relaxation zone volume in the HW of stopes, serves as parameters for assessing the geomechanical efficacy of the designs under scrutiny. The evaluation process is implemented in FISH, FLAC3D's internal programming language.

3.4 Graphical User Interface (GUI)

The graphical user interface (GUI) for the program was produced using the Python library package PySimpleGUI. For the developed program, a main window is used, and the input parameters are arranged into six distinct tabs, according to the program's sections. The tabs are as follows: "Files," "Geometric Parameters," "Economic Data," "Geomechanics," "Genetic Algorithm," and "Execute." Four buttons are always visible, regardless of the selected tab: "Optimize," "Cancel," "Open Form," and "Save Form." Figure 1 below shows the interface of the program's main window and the progress bar screen in front, during its execution.
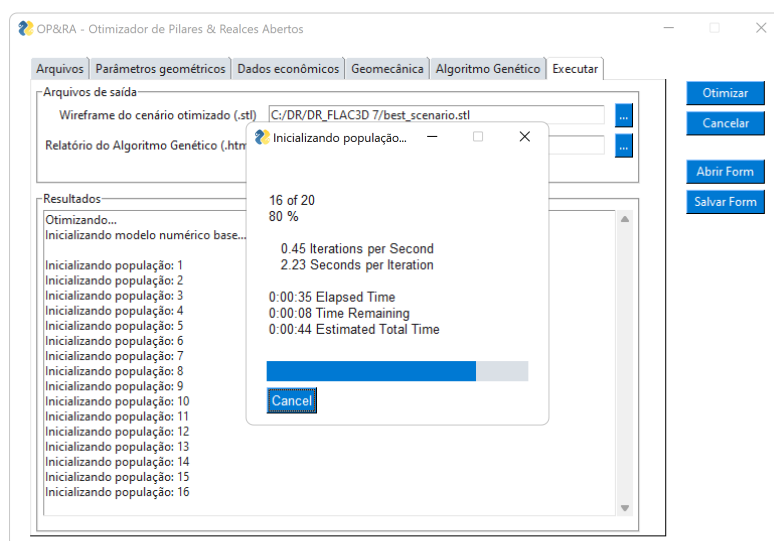

Figure 1. Program GUI with six tabs for inputting parameters and progress screen during execution.

4   CASE STUDY

The examined case study pertains to an extension project within an underground gold mine characterized by marginal ore content and a projected lifespan of 2 years. Given the project's short duration and economic considerations, the adopted method is a top-down sublevel open stope approach. The average depth of the deposit reaches 200 m, with the ore body exhibiting dips between 60-70 degrees and a relatively narrow thickness ranging from 5-7 m. Sublevel spacing is set at 15 meters, while the minimum permissible stope length is determined to be 7 m, driven by economic and operational considerations.

4.1 Geomechanical properties

The properties pertinent to the case study are detailed in Table 2, sourced from the geomechanical evaluation provided by the company. Uniform properties were chosen for the HW domain throughout the entire zone, given the absence of a clearly defined contact in the HW fault zone. Alternatively, distinct

XX ICongresso Brasileiro de Mecânica dos Solos e Engenharia Geotécnica
X Simpósio Brasileiro de Mecânica das Rochas
X Simpósio Brasileiro de Engenheiros Geotécnicos Jovens
24 a 27 de setembro de 2024 – Balneário Camboriú/SC

properties could have been applied for the fault zone as a subdomain.

In determining the magnitude of in situ stress, the geological setting was deemed relatively stable, with minimal significant tectonic influences. Equations akin to those by Brown and Hoek (1978) and Sheorey (1994) were utilized for estimating in situ stresses. An average specific weight of 0.028MN/m^3 was employed in calculations. The horizontal stress component (σ_h) was derived by applying a factor (k) to the vertical stress (σ_v). Hence, it was assumed that the major principal stress (σ_1) and the intermediate principal stress (σ_2) were equal in magnitude and horizontal, while the minor principal stress (σ_3) was vertical. Given an average modulus of elasticity of 25 GPa and a depth of 200 m, a value of 1.3 was assigned to (k).

Table 2. Geomechanical input parameters

Domain	Specific Weight (t/m^3)	GSI	Bulk modulus (GPa)	Shear modulus (GPa)	Mohr-Coulomb	
					Friction angle (°)	Cohesion (MPa)
Hangingwall	2.75	55	21.9	8.9	40.0	1.1
Ore body	2.78	70	46.4	13.1	46.9	1.4
Footwall	2.63	65	44.1	18.1	47.0	2.0

4.2 Empirical stability analysis

To evaluate stope stability, empirical analyses were conducted referencing works by Potvin (1988) and Nickson (1992). Additionally, the ELOS factor, as proposed by Clark and Pakalnis (1997), was utilized to estimate HW dilution. The stability number (N') was assumed to have a mean value of 20. Stope dimensions were varied with lengths ranging from 7 to 25 m and heights from 15 to 60 m, considering up to 4 levels of interconnected stopes. The minimum hydraulic radius (HR) observed was 2.5 m, while the maximum reached 8.8 m. Consequently, stopes were deemed stable without the need for support when the HR was up to 7 m. For HR values between 7 and 13 m, cablebolt support was deemed necessary. For instance, with an HR of 10 m, an ELOS factor ranging from 0.5 to 1 m could be anticipated at the HW.

Pillar stability analysis followed the methodology by Lunder and Pakalnis (1997). Pillar height was fixed at 15 m, while the length varied from 5 to 10 m. Average stress within the pillars ranged from 15 to 20 MPa, with uniaxial compressive strength measured at 90 MPa. In these conditions, factors of safety were 1.4.

4.3 Operational and economic parameters

The economic parameters considered for the case study are from 2021. The operational parameters considered for optimization can also be observed in Table 3.

Table 3. Economic and operational input parameters entered by the user in the program's GUI.

Input parameters	Value
Gold price ($/g)	55.0
Mining recovery (%)	90.0
Process recovery (%)	93.0
Max. accepted dilution (%)	10.0
Max. accepted pillar failure (%)	10.0
Mining cost ($/t)	16.5
Transport cost ($/t/m)	0.00014
Process cost ($/t)	18.6
General & admin. cost ($/t)	18.1
Gold refining ($/g)	0.5
Royalties (% gross value)	0.015
Secondary support cost ($/m^3 of dilution)	1.0
Secondary support efficiency (%)	70
Pillar support cost ($/m^3 of failed pillar)	0.9
Minimum pillar length (m)	5
Maximum pillar length (m)	10
Minimum stope length (m)	7
Maximum stope length (m)	25

XX ICongresso Brasileiro de Mecânica dos Solos e Engenharia Geotécnica
X Simpósio Brasileiro de Mecânica das Rochas
X Simpósio Brasileiro de Engenheiros Geotécnicos Jovens
24 a 27 de setembro de 2024 – Balneário Camboriú/SC

COBRAMSEG 2024
XXI Congresso Brasileiro de Mecânica dos Solos e Eng. Geotécnica
X Simpósio Brasileiro de Mecânica das Rochas
X Simpósio Brasileiro de Engenheiros Geotécnicos Jovens

5   RESULTS AND DISCUSSION

The subsequent section outlines optimization procedures performed in a case study, contrasting outcomes obtained through the proposed methodology with those derived from the engineer's design. Figure 2 illustrates the geometry of the stopes and pillars layout as per the engineer's design, analyzed using FLAC3D. The layout appears relatively uniform, featuring larger stopes situated predominantly in the central area of the mining panel. A total of 30 stopes and 31 pillars were considered in the analysis.
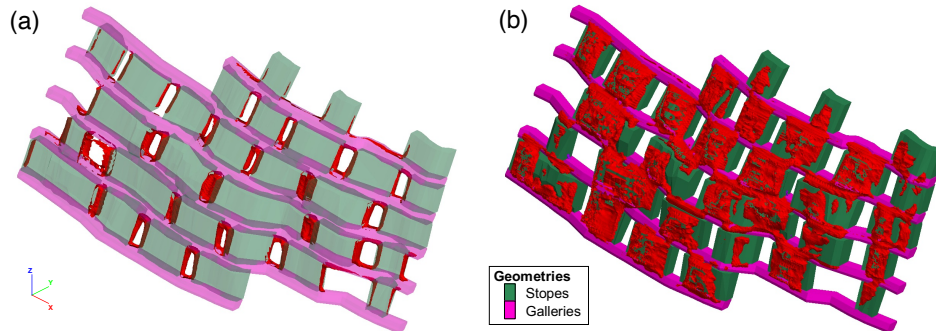

Figure 2. Base case of stopes and pillars layout: (a) Isovolume of pillar failures (red color); (b) Isovolume of potential HW dilution (red color).

5.1 Optimal scenario considering the proposed methodology

Optimization parameters encompassed an initial population of 20 individuals, a maximum of 1000 iterations, patience set at 200, and a mutation probability of 0.5. The algorithm completed the maximum iterations, exhibiting a higher evolution rate within the initial 200 generations, followed by an intermediate rate from 200 to 750 generations, and a slower evolution from 750 to 1000 generations. The optimization process required approximately 126 hours of computational time on a relatively modern computer.

The proposed methodology yielded an optimal scenario with ore production totaling 263 kt, boasting an average grade of 1.55 g/t, resulting in 13,049 contained ounces and a global recovery rate of 70.4%. The optimized geometry presented a dilution potential of 24.4%, which, considering a 70% efficiency rate of HW support, translated to an actual dilution of 14.3%, mirroring the engineer's design.

Pillar failure percentage stood at 3.4%, marking a 3.4-fold decrease compared to the engineer's design. Gross income was estimated at $18.7 million, while costs amounted to $14.8 million, resulting in a net profit of $3.9 million. By eliminating HW support, the actual dilution matched the maximum potential dilution obtained from the numerical model at 24.3%, leading to a net profit of $2.6 million. Thus, a 22% net profit improvement was observed without HW support, while an 8% improvement was realized with a 70% support efficiency. The optimized stopes and pillars geometry, analyzed in FLAC3D, is depicted in Figure 3.
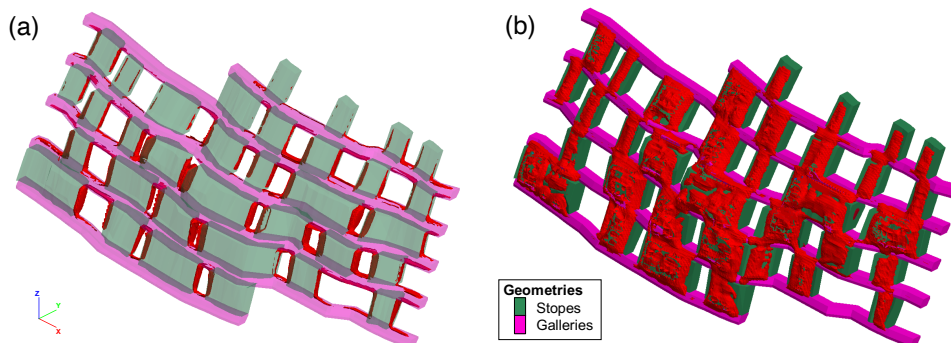

Figure 3. Algorithm result of stopes and pillars layout: (a) Isovolume of pillar failures (red color); (b) Isovolume of potential HW dilution (red color)

Notably, the arrangement exhibits relative irregularity, featuring larger stopes concentrated in the central area of the panel and smaller stopes situated in the upper levels. A total of 34 stopes, with an average length of 12.7 m, and 37 pillars, with an average length of 8.2 m, were considered in the analysis.

XX ICongresso Brasileiro de Mecânica dos Solos e Engenharia Geotécnica
X Simpósio Brasileiro de Mecânica das Rochas
X Simpósio Brasileiro de Engenheiros Geotécnicos Jovens
24 a 27 de setembro de 2024 – Balneário Camboriú/SC

COBRAMSEG 2024
XXI Congresso Brasileiro de Mecânica dos Solos e Eng. Geotécnica
X Simpósio Brasileiro de Mecânica das Rochas
X Simpósio Brasileiro de Engenheiros Geotécnicos Jovens

6   CONCLUSIONS AND FUTURE WORK

This study presents a novel integrated methodology that effectively combines economic and geomechanical parameters to optimize stope and rib pillar layouts in sublevel open stope mining. By employing a genetic algorithm, we have demonstrated a significant improvement in net profit and geomechanical performance compared to traditional engineering design methods.

The proposed profit function, which incorporates mining recovery, process recovery, and various cost factors, allows for a comprehensive evaluation of the economic viability of stope and pillar configurations. The case study results indicate an 8% increase in net profit with hanging wall support and a 22% increase without it, highlighting the methodology's robustness in different scenarios.

Future efforts will explore the integration of geomechanical models to improve results by considering variations throughout the rock mass. Furthermore, improvements are anticipated through the inclusion of various failure criteria and plastic behavior. Testing the methodology on different ore bodies in more complex geological environments or different mining methods will help validate its versatility and robustness.

ACKNOWLEDGMENTS

REFERENCES

Alford, C. (2006) *Optimization in underground mine design*. PhD thesis, Department of Mathematics and Statistics, The University of Melbourne

Brown, E.T., Hoek, E. (1978) Trends in relationships between measured in-situ stresses and depth. *Int. J. Rock Mech. Min. Sci. & Geomechanics Abstracts* 15, 211–215

Castro, L.A.M., Bewick, R.P., Carter, T.G. (2012) An overview of numerical modelling applied to deep mining. In: Sousa, L.R., Jr., E.V., Fernandes, M.M., Azevedo, R. (eds.) *Innovative Numerical Modelling in Geomechanics*, pp. 405–426. CRC Press, London

Clark, L., Pakalnis, R. (1997) An empirical design approach for estimating unplanned dilution from open stope hangingwalls and footwalls. In: *Proc. of the 99th Annual General Meeting*. CIM

Cordova, D.P., Zingano, A.C., Gonçalves, I.G. (2022) Unplanned dilution back analysis in an underground mine using numerical models. *REM - International Engineering Journal* 75, 379–388

Diederichs, M.S. (1999) *Instability of hard rockmasses, the role of tensile damage and relaxation*. PhD thesis, University of Waterloo.

Furtney, J. (2020) *Itasca: Python package*. https://pypi.org/project/itasca/ Accessed 28 August 2023

Heidarzadeh, S., Saeidi, A., Rouleau, A. (2019) Evaluation of the effect of geometrical parameters on stope probability of failure in the open stoping method using numerical modeling. *Int. J. Min. Sci. Technol.* 29

Itasca Consulting Group Inc. (2005) *Flac 5 Manual*, p. 3058. Itasca, Minneapolis

Lunder, P.J., Pakalnis, R.C. (1997) A determination of the strength of hard-rock mine pillars. *CIM* 90, 51–55

Mitchell, M. (1998) *An Introduction to Genetic Algorithms*. The MIT Press, London.

Napa-Garcia, G.F., Câmara, T.R., Torres, V.F.N. (2019) Optimization of room-and-pillar dimensions using automated numerical models. *Int. J. Min. Sci. Technol.* 29, 797–801

Nickson, S.D. (1992) *Cable support guidelines for underground hard rock mine operations*. PhD thesis, University of British Columbia.

Potvin, Y. (1988) *Empirical open stope design in Canada*. PhD thesis, University of British Columbia.

Sari, Y.A., Kumral, M. (2020) A planning approach for polymetallic mines using a sublevel stoping technique with pillars and ultimate stope limits. *Engineering Optimization* 52, 932–944

Sheorey, P.R. (1994) A theory for in situ stresses in isotropic and transversely isotropic rock. *Int. J. Rock Mech. Min. Sci. & Geomechanics Abstracts* 31, 193